Geotextiles and Geomembranes 44 (2016) 188–200

Contents lists available at ScienceDirect

Geotextiles and Geomembranes

journal homepage: www.elsevier.com/locate/geotexmem

Centrifuge evaluation of the time-dependent behavior of geotextile-reinforced soil walls

Carina Maia Lins Costa [a, *], Jorge Gabriel Zornberg [b, 1], Benedito de Souza Bueno [c, 2], Yuri Daniel Jatobá Costa [a, 3]

[a] Federal University of Rio Grande do Norte, Campus Universitário Lagoa Nova, Natal, RN 59078-970, Brazil
[b] The University of Texas at Austin, Department of Civil Architectural and Environmental Engineering, 301 E. Dean Keeton, Austin, TX 78712-0280, USA
[c] University of São Paulo, Av. Trabalhador São Carlense, 400, 13566-590, São Carlos, SP, Brazil

ARTICLE INFO

Article history:
Received 13 August 2014
Received in revised form
23 August 2015
Accepted 5 September 2015
Available online xxx

Keywords:
Geosynthetics
Geotextiles
Centrifuge
Reinforced soil
Creep

ABSTRACT

This paper presents the results of a centrifuge study performed to investigate the time-dependent behavior of geotextile-reinforced soil walls. To this effect, reduced-scale centrifuge models were built using nonwoven fabrics as reinforcement elements and Monterey no. 30 sand as backfill. Digital image analysis techniques were used to quantify the internal displacements within the reinforced zone, where sand markers had been placed along the reinforcement layers. A sigmoid function was found to provide adequate fit to raw displacement data, allowing estimation of the strain distribution along the reinforcement layers. This investigation includes an initial series of centrifuge models designated as "Short-term" tests, which were loaded to failure by continuously increasing the acceleration imparted to them. In addition, a series of models designated as "Long-term" tests were conducted by subjecting them to constant accelerations corresponding to 25%, 40%, 60% and 80% of the g-level at failure obtained from the "Short-term" tests. The results revealed that walls subjected to constant acceleration showed a time-dependent behavior that adversely affected their stability. Considerable time-dependent deformations were observed to occur during the "Long-term" tests. That is, time-dependent deformations in the reinforcements, quantified using geosynthetic samples tested in isolation, were found to also develop under confinement in the centrifuge models. In particular, creep failure was observed in the "Long-term" models subjected to comparatively high levels of constant acceleration. The time-dependent deformations from confined geotextiles tested in the centrifuge testing program were compared against the results from unconfined geotextiles tested in a conventional creep testing program. The time to failure defined using data from centrifuge tests was found to be consistent with that obtained from conventional creep tests. The soil used in the centrifuge models in this study, frequently considered as having negligible creep, was ultimately found not to prevent the development of time-dependent deformations.

1. Introduction

Geosynthetic-reinforced soil (GRS) walls have been adopted worldwide in earth retention projects because of the important technical and economical advantages they offer in relation to conventional retaining structures. However, a concern regarding the adoption of these systems has been the potential of geosynthetics to exhibit a time-dependent behavior under sustained load. Evaluation of the time-dependent behavior of geosynthetics has been typically done by characterizing their rheologic mechanisms such as creep and stress relaxation. Creep involves the development of time-dependent deformations in a geosynthetic under constant loading. On the other hand, stress relaxation corresponds to the time-dependent decrease in unit tension in a geosynthetic subjected to imposed constant strains.

Assessment of the time-dependent behavior of geosynthetics is important for the design of reinforced soil structures since reinforcements are expected to remain under tension during the

* Corresponding author. Tel.: +55 84 33422496; fax: +55 84 3215 3703.
E-mail addresses: cmlins@gmail.com, carina@ct.ufrn.br (C.M.L. Costa), zornberg@mail.utexas.edu (J.G. Zornberg), bsbueno@sc.usp.br (B.S. Bueno), ydjcosta@ct.ufrn.br (Y.D.J. Costa).
[1] Tel.: +1 512 232 3595; fax: +1 512 417 6548.
[2] Tel.: +55 16 3373 6501; fax: +55 16 3373 9509.
[3] Tel.: +55 84 33422496; fax: +55 84 3215 3703.

http://dx.doi.org/10.1016/j.geotexmem.2015.09.001
0266-1144/

entire design life of the structure. Excessive deformations and even creep failure has been identified as possible consequences of the time-dependent behavior of the geosynthetic-reinforced soil structures. Typically, evaluation of the long-term behavior of a GRS structure is based on results from creep tests conducted on geosynthetic specimens tested in isolation, without the confinement of soil. Creep tests conducted at elevated temperature have been used to accelerate the generation of time-dependent data (Zornberg et al., 2004; Bueno et al., 2005; Kongkitkul and Tatsuoka, 2007; Jones and Clarke, 2007; Yeo and Hsuan, 2010). However, the long-term deformation of actual GRS walls has been expected to be affected by the interaction between the geosynthetic reinforcement and the confining soil.

Initial studies on the evaluation of the effect of soil confinement on the creep behavior of geosynthetic reinforcements were conducted using devices that allowed testing of geotextiles placed between two layers of soil. Tensile forces were applied directly to the reinforcement after having applied a target confining stress to the soil. This technique has been conducted primarily for the case of nonwoven geotextiles with the objective of assessing possible restriction in the movement of the fibers and their alignment in the direction of loading. Using this type of device, McGown et al. (1982) reported a considerable reduction in the time-dependent deformations of nonwoven geotextiles confined between layers of sand. However, significant smaller reductions were subsequently reported by Levacher et al. (1994) and Wu and Hong (1994).

The need to also consider the rheologic behavior of the confining soil on the overall long-term behavior of reinforced soil structures, rather than relying solely on the rheologic behavior of geosynthetic reinforcements has been identified (e.g. Liu et al., 2009; Li et al., 2012). However, only a limited number of experimental evaluations has been conducted so far on the time-dependent behavior of the interaction between soil and reinforcement (e.g. Wu and Helwany, 1996; Helwany and Shih, 1998; Ketchart and Wu, 2002). The approach in these studies involved confining geosynthetics between soil layers and applying a constant vertical stress to the soil which, in turn, mobilized the axial load in the reinforcements. In this testing approach, both soil and reinforcement can exhibit time-dependent deformations, while accounting for their interaction. In particular, Wu and Helwany (1996) concluded that if the confining soil exhibits less tendency to creep than the geosynthetic, the soil would then impose a restraining effect on the geosynthetic deformation. The interaction mechanisms on the time-dependent response were reported to be associated to the shear strength properties of the interface between the two materials.

The use of reduced scale models of GRS walls tested in a centrifuge environment provides an alternative approach for evaluating interactions between soil and geosynthetic reinforcements. However, only preliminary attempts have been made in this regard. Mitchell et al. (1988) conducted centrifuge tests using reduced-scale models built using sand and nonwoven polyester fabrics as reinforcement. Some models were tested under constant acceleration for limited periods of time. While reinforcement strains were not measured, visual observation of the models revealed the development of time-dependent deformations.

The evaluation of full-scale instrumented walls also constitutes an important approach to investigate the long-term behavior of GRS walls. Some studies have recently provided constitutive rheological models to describe the time-dependent behavior of geosynthetics (e.g. Kongkitkul et al., 2010; Kongkitkul et al. 2014) that can be used to simulate the interactive soil-geosynthetic response of instrumented GRS structures. However, in most of the reported studies involving the observation of full-scale geosynthetic walls, either the structure's time-dependent behavior has not been monitored or the collected displacements were negligible or insufficient for adequate long-term assessment. A notable exception is the work reported by Allen and Bathurst (2002a), which shows a detailed re-evaluation of data presented by Bathurst and Benjamim (1990) and Bathurst et al. (1993). Full scale GRS walls, built using sand and polypropylene geogrids, showed significant deformations over time after subjecting them to comparatively high surcharge loads. The strain rate in these walls, during a selected time-span, was found to exceed that predicted using results from conventional creep tests conducted using reinforcements tested in isolation. While the authors reported that this time-dependent behavior may be attributed to soil-reinforcement interaction, the mechanism of this interaction was not fully addressed.

In summary, only limited information is currently available in the technical literature on the time-dependent deformations of GRS that account for soil-reinforcement interaction. Accordingly, this paper presents the results of a series of centrifuge model tests performed to investigate time-dependent interaction between soil and geotextiles in GRS walls. Two series of centrifuge tests were performed as part of this investigation, which involved reduced-scale walls built using nonwoven fabrics as reinforcement and sand as backfill. The first series of tests ("Short-term" tests) involved reduced-scale models loaded to failure by continuously increasing the centrifugal acceleration in order to characterize the g-level at failure that corresponds to a given wall configuration. The second series of tests ("Long-term" tests) involved models monitored over time under constant acceleration with the aim of evaluating the time-dependent response of the GRS walls under sustained loading. It should be noted that the objective of the centrifuge investigation conducted in this study was not to simulate particular prototypes. Instead, the centrifuge approach was adopted to identify time-dependent interaction mechanisms between soil and reinforcement. The use of centrifuge modeling allowed the study of the long-term behavior of GRS walls structures under stress levels that are higher than those mobilized under typical working stress conditions.

2. Description of centrifuge models

2.1. General model characteristics

Reduced-scale geosynthetic-reinforced walls were tested using a 15 g-ton geotechnical centrifuge available at the University of Colorado at Boulder. The centrifuge models were built using sand as backfill and interfacing fabrics as reinforcement simulants. A strong box with plan dimensions of 419 mm × 203 mm and a height of 300 mm was used to house the models. A transparent Plexiglas plate lined with a Mylar sheet was used as one of the side walls of the box to enable in-flight visualization of the models during testing. The other walls of the strong box consisted of aluminum plates lined with Teflon in order to minimize wall side friction.

Fig. 1 shows the geometry of the reinforced walls models, which were built to a height of 229 mm on a 25.4 mm-thick foundation layer. The facing of the walls was flexible (i.e. built using wrapped-around reinforcements), with an inclination of 85° to the horizontal. Air-dried Monterey No. 30 sand was used as backfill material and for the foundation soil. The sand was air-pluviated under controlled conditions to produce a target relative density of 70% in the reinforced soil zone and of 100% in the foundation layer. The general procedure followed for construction of these models is consistent with that reported by Zornberg et al. (1997). Twelve equally spaced reinforcement layers were used in the models, which corresponded to a vertical reinforcement spacing of 19 mm. All models were built using 203 mm-long reinforcements. The layer

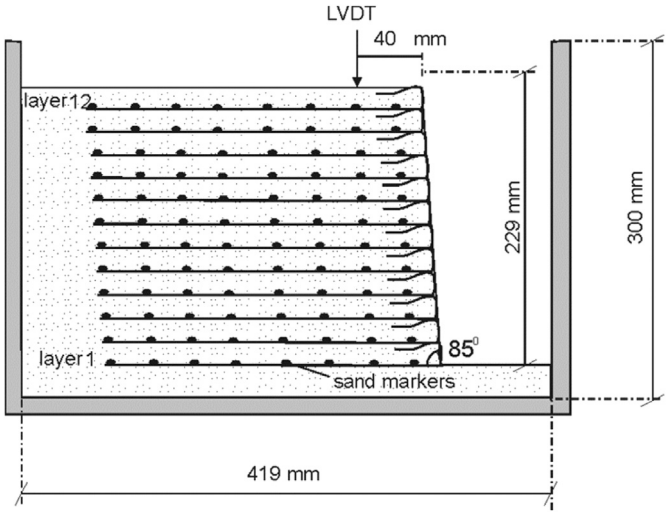

Fig. 1. Layout of centrifuge models.

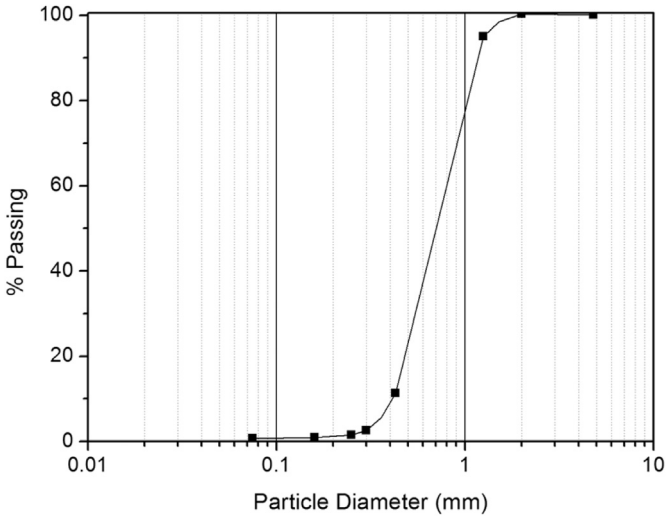

Fig. 3. Gradation curve for Monterey No. 30 sand.

designation adopted herein is also shown in Fig. 1, with Layer 1 corresponding to the bottom reinforcement layer and Layer 12 corresponding to the top one. Fig. 2 presents a view of one of the models inside de centrifuge and ready for testing.

Instrumentation during the centrifuge testing included a linear variable displacement transformer (LVDT) to monitor vertical settlements at the top of the model (Fig. 1) and thermocouples to monitor internal temperature. In addition, black sand markers were placed along the Plexiglas wall at the elevation of each reinforcement layer in order to measure the displacements along the reinforcement layers by continuously monitoring the entire wall section through the Plexiglas wall using digital images captured in-flight.

2.2. Description of the materials

2.2.1. Backfill soil

Monterey no. 30 is an uniformly graded sand that classifies as SP according to the Unified Soil Classification System (USCS). It consists predominantly of quartz particles with small amounts of feldspars and other minerals (Zornberg et al., 1997). The particle shape is rounded to subrounded. Fig. 3 presents the gradation curve for Monterey no. 30 sand, which results in a coefficient of uniformity of 1.8, a coefficient of curvature of about 1.0. The minimum and maximum dry unit weights are 14.8 kN/m^3 and 16.7 kN/m^3, respectively, which were obtained in accordance with ASTM D4254 (2014) and ASTM 4253 (2014). The corresponding maximum and minimum void ratios are 0.76 and 0.56, respectively.

Shear strength properties of the backfill sand were obtained from triaxial tests. For the selected relative density used in the models (D_r = 70%), the sand showed a peak friction angle (ϕ) of 36.4°.

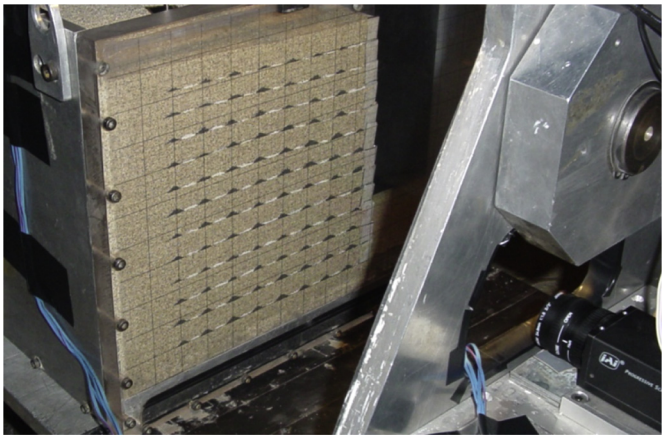

Fig. 2. View of one of the centrifuge models ready for testing.

2.2.2. Geotextile reinforcements

Two types of nonwoven geotextiles were used as geosynthetic reinforcements, designated herein as Geotextiles A and B. The material types and manufacturing techniques of the selected model reinforcements are consistent with those in commercially available geosynthetics. The scaling laws for centrifuge testing of reinforced soil structures establish that the reinforcement strength in the model should be N times weaker than that in the prototype (Zornberg et al., 1997), where N is the in-flight g-level. In addition, the stiffness of the reinforcements used in the models should equal 1/N times the stiffness in the prototype reinforcement. The scaling factor for time in centrifuge studies has been assumed to equal one for problems involving rheologic phenomena (e.g. creep), which is the focus of this study. While the centrifuge wall models built in this study do not aim at modeling the behavior of a specific prototype structure, the selected model reinforcements showed a tensile strength that was small enough to reach in-flight internal failure of the models. The characteristics of the geotextile reinforcements used in this study are discussed next.

Geotextile A is a nonwoven interfacing fabric manufactured by the Pellon Division of Freudenberg Nonwovens and commercially designated as Pellon Sew-in. The material is a polyester fabric with a mass per unit area of 23 g/m^2. Wide–width tensile tests were performed in accordance to ASTM D4595 (2011) to quantify the unconfined ultimate tensile strength of the geotextile. Geotextile A is highly anisotropic in terms of tensile strength, having a lower tensile strength in the cross-machine direction than in the machine direction. Since all centrifuge models were built using the fabrics oriented in the cross-machine direction, geotextile tensile strength was evaluated along this direction. Fig. 4 presents the results of a series of tensile tests, which rendered an average ultimate tensile strength of 0.033 kN/m in the cross-machine direction.

Fig. 5 shows the results of a series of conventional creep tests conducted without soil confinement in accordance with ASTM

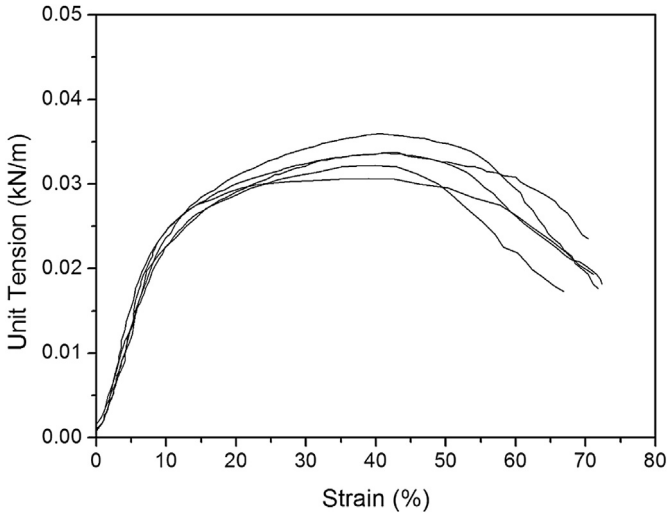

Fig. 4. Results of tensile tests conducted in the cross-machine direction using Geotextile A.

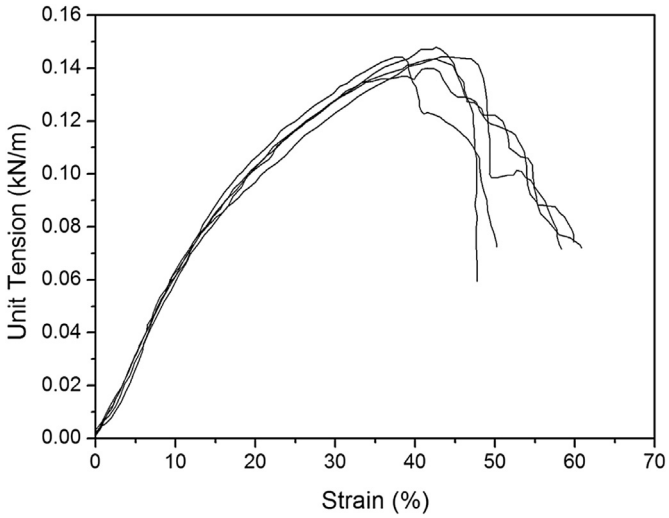

Fig. 6. Results of tensile tests conducted in the cross-machine direction using Geotextile B.

D5262 (2012). The applied load levels correspond to 25%, 40%, 60%, and 80% of the material ultimate tensile strength (T_{ult}). Multiple specimens were tested in most of the load levels in order to assess repeatability of the test results. Each of the test shown in Fig. 5 were conducted using different specimens. In particular, three repeat tests were conducted for the highest load level in order to better characterize the creep failure conditions. Time to failure ranged from 2 to 5 h for the various specimens tested under a constant load corresponding to 80% of the ultimate tensile strength.

Geotextile B is a polypropylene nonwoven fabric with a mass per unit area of 12 g/m^2 manufactured by BBA Nonwovens. The material is not commercially available and was especially manufactured for the propose of this research. As in the case of Geotextile A, the tensile strength of Geotextile B was also lower in the cross-machine than in the machine direction. However, anisotropy in Geotextile B was less significant than that in Geotextile A. Fig. 6 presents typical tensile test results of specimens of Geotextile B tested in the cross-machine direction. The unconfined ultimate tensile strength of Geotextile B, defined using wide-width tensile tests (ASTM D4595, 2011), is 0.144 kN/m.

Conventional creep tests, conducted in accordance to ASTM D5262 (2012), were also performed using Geotextile B. The results are presented in Fig. 7. Multiple specimens were also tested in most of the load levels in order to assess the repeatability of the test results. The geotextile specimens loaded to 80% of its ultimate tensile strength showed a time to creep failure ranging from 1.0 to 1.6 h.

3. Scope of the centrifuge testing program

As summarized in Table 1, two series of centrifuge tests were performed as part of this investigation. Models F1 to F6, designated herein as “Short-term” tests, were loaded to failure by continuously increasing the centrifugal acceleration. More specifically, the g-level was increased during testing by applying increments of approximately 4 g. The main purposes of the “Short-term” tests was to identify g-level at failure as well as defining the rupture

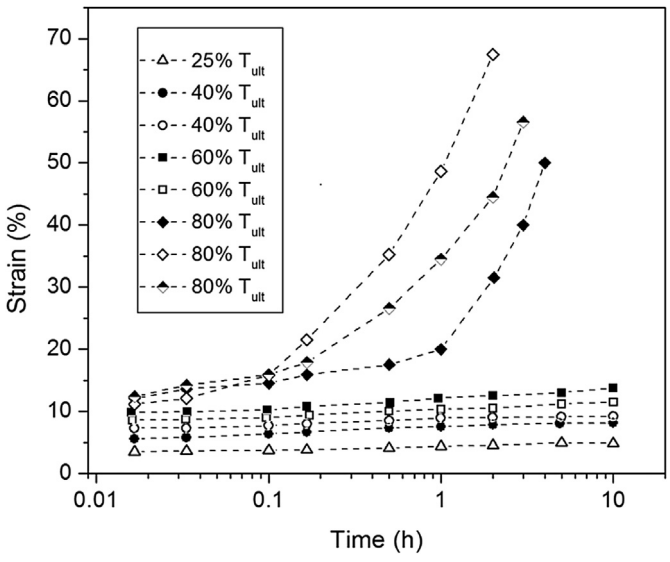

Fig. 5. Results of conventional creep test conducted using Geotextile A.

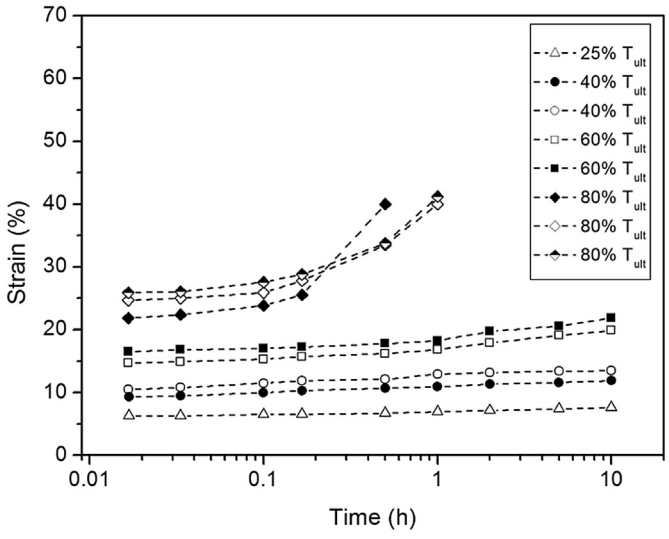

Fig. 7. Results of conventional creep test conducted using Geotextile B.

Table 1
Summary of centrifuge tests.

Model	Test procedure	Geotextile	Centrifugal acceleration level in "Long-term" tests (% N_f[a])
F1	"Short-term" tests	A	–
F2		A	
F3		A	
F4		A	
F5		B	
F6		B	
C1	"Long-term" tests	A	25
C2		A	40
C3		A	60
C4		A	80
C5		B	25
C6		B	40
C7		B	60
C8		B	80

[a] Average value for "Short-term" tests, $N_f = 20$ for Geotextile A and $N_f = 48.5$ for Geotextile B (see Table 3).

mechanisms of the structure. All tests were conducted using models constructed using the layout shown in Fig. 1, although using the two different types of geotextiles (A and B) characterized in this study. Multiple tests were conducted following the same testing procedure in order to evaluate the repeatability of the test results. In particular, models F1, F2 and F3 are identical and were constructed using Geotextile A. As will be subsequently discussed, Model F4 was conducted to elucidate specific aspects related to the failure mechanism of the walls. Finally, Models F5 and F6 are identical and were built using Geotextile B.

The second series of tests (Models C1 to C8) involved reduced-scale walls subjected to constant accelerations selected to be equal to 25, 40, 60 and 80% of the g-level corresponding to failure in the "Short-term" models tested in the previous series. The time-dependent deformations of these models were generally monitored during 10 h in order to evaluate the long-term behavior of the walls under constant centrifugal acceleration.

4. Determination of the strain distribution along geosynthetic reinforcements

The images collected in-flight during centrifuge testing were processed using the approach described by Zornberg and Arriaga (2003). Specifically, the displacements of sand markers were obtained by analyzing the digital data from photographs collected during the tests. This analysis involved the determination of the spatial coordinates of the center of mass of each sand marker. The markers closest to the wall face at each reinforcement level were adopted as references to determine the relative distances between markers during the progress of each centrifuge test.

The displacement data collected from images at different times were fitted to a sigmoid curve following the procedure reported by Zornberg (1994). The sigmoid function used to fit the relative displacement can be represented as:

$$d = \frac{1}{a + b \cdot e^{-cx}} \tag{1}$$

where d is the marker relative displacement at a given time, x is the original distance between the marker and the corresponding reference marker (i.e. the distance from each marker to the face), e is the natural logarithm base, and a, b, and c are parameters defined by fitting the displacement data to the sigmoid curve using the least squares technique.

The strain distribution for each geotextile reinforcement was subsequently obtained as the derivative of the displacement distribution function. The strain distribution calculated using this procedure shows zero strain values at the face of the wall and at the embedded end of the reinforcements. This trend in reinforcement strains is consistent with that reported for geosynthetic-reinforced structures with extensible facing. The peak strain value (i.e. maximum strain value) and its location from wall face in each reinforcement layer can be predicted using the parameters a, b, and c, used to fit the displacement data. Specifically, these values can be calculated as follows (Zornberg and Arriaga, 2003):

$$\varepsilon_{max} = c/4a \tag{2}$$

$$x_{max} = \frac{1}{c} \ln \left(\frac{b}{a}\right) \tag{3}$$

where ε_{max} is the magnitude of the peak strain in each reinforcement layer and x_{max} is the location, measured from the wall face, of the peak strain.

In summary, the analysis of digital image conducted in this study involved tracking the location of markers in each reinforcement layer, subsequent determination of the displacements of each marker and final prediction of the strain distribution along each reinforcement layer using the sigmoid curves defined from displacement information. Additional details of this procedure is reported by Zornberg and Arriaga (2003).

5. Analysis of the centrifuge test results

5.1. Results from the "Short-term" test series

The settlements measured at the crest of the models during the "Short-term" tests, as a function of the imposed g-level, are presented in Fig. 8. As previously mentioned, the settlements were measured using an LVTD positioned 40 mm from the wall face (Fig. 1). As shown in Fig. 8, the results obtained for multiple repeats of "Short-term" tests, conducted using models constructed with Geotextile A, were remarkably similar. Similarly good repeatability was obtained for tests conducted using models constructed with Geotextile B. This provides evidence of the consistency of the experimental procedures adopted in this study. The curves in Fig. 8 show an approximately bi-linear shape, with an initial portion of comparatively small settlement changes, followed by a portion of large settlement changes with increasing g-levels. An additional increase in acceleration beyond the maximum g-level values shown in Fig. 8, resulted in collapse of each model. Collapse of the walls was characterized by the development of an active wedge behind wall facing, sliding along a well-defined failure surface. The magnitude of the settlements after collapse exceeded the range of the LVDT.

Fig. 9 shows a typical relative displacement profile for one of the reinforcement layers, as obtained for increasing values of centrifugal acceleration (Layer 10 of model F3). The values of centrifugal acceleration in the figure are shown as a percentage of g-level that led the model to failure (N_f). As shown in Fig. 9, the sigmoid function (Equation (1)) is found to fit well the relative displacement data. Table 2 presents the equation and the coefficient of determination (R^2) for the curves shown in Fig. 9. The value of R^2 ranges from 0.97 to 0.99. The sigmoid function was found to fit well the displacement data for the relative displacements in all reinforcement layers of the multiple centrifuge tests. The minimum value of R^2 among all the fitted sigmoid curves was 0.90 for "Long-term" and 0.97 for "Short-term" tests.

Fig. 10 shows a typical strain distribution predicted for one of reinforcement layers, as obtained for increasing values of

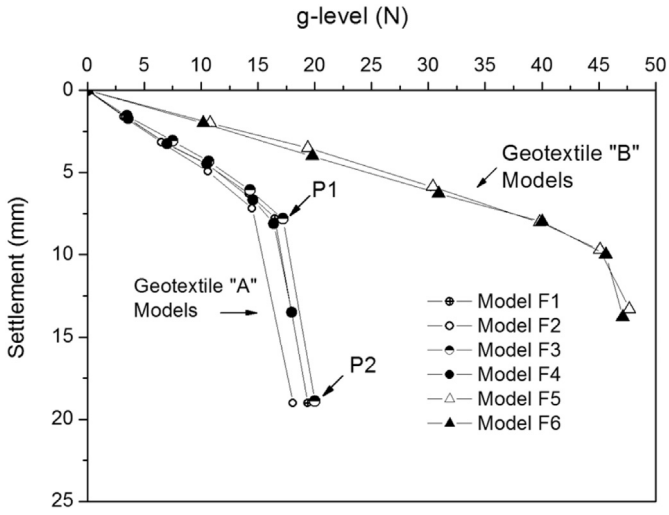

Fig. 8. Settlements at the crest of the walls for increasing g-level ("Short-term" tests).

centrifugal acceleration (Layer 10 of Model F3). The curves presented in Fig. 10 were obtained as the derivative of the displacement distribution function, as previously described in Section 4. As show in Fig. 10, the predicted pattern of the strain distribution, tended to zero towards the wall face and towards the end of the reinforcements. Similar patterns were obtained for all reinforcement layers in the multiple centrifuge models (both "Short and Long-term" tests) and for models constructed using both Geotextile A and B. As anticipated, an increase in the magnitude of the peak strain was obtained for each reinforcement layer with increasing g-levels.

The thermocouples installed within the models indicated only slight temperature variations, which were considered negligible for the purposes of this study.

5.1.1. Evaluation of the g-levels at failure

Evaluation of the g-level at failure, as obtained in the "Short-term" test series, provides relevant information for the subsequent interpretation of the "Long-term" behavior of the reduced-scale walls. In this study, the g-level at failure of "Short-term" models was defined as the centrifugal acceleration that led to rupture of at least one of the reinforcement layers. Images collected in-flight during centrifuge testing as well as visual inspections of the models after testing were used to determine the g-level at failure of the "Short-term" models. The pattern of the settlement versus g-level curves obtained in the centrifuge tests as well as the pattern of the geotextile tensile test curves were also evaluated to accurately establish the g-level at failure.

Table 2
Fitting functions and coefficient of determination (R^2) for sigmoid curves shown in Fig. 9.

g-level (as a fraction of N_f)	Equation for fitted curve d (mm)	R^2
95%	$d = \frac{1}{0.0385+3.39 \cdot e^{-0.0576 \cdot x}}$	0.99
82%	$d = \frac{1}{0.0912+5.18 \cdot e^{-0.0509 \cdot x}}$	0.97
68%	$d = \frac{1}{0.1361+25.70 \cdot e^{-0.0648 \cdot x}}$	0.98
51%	$d = \frac{1}{0.2232+44.98 \cdot e^{-0.0669 \cdot x}}$	0.99
36%	$d = \frac{1}{0.3344+27.32 \cdot e^{-0.0578 \cdot x}}$	0.99

The pattern of the settlement versus g-level curves, as shown in Fig. 8 presents two characteristics points, P1 and P2 that are typical for the response of the centrifuge models constructed using Geotextile A (points are identified for Model F3 in the figure). For g-levels beyond point P1, significant increases in settlement were observed for increasing centrifugal accelerations. A somewhat equivalent pattern can be identified upon inspection of tensile test results for Geotextile A, as presented in Fig. 4 and idealized in Fig. 11. Specifically, tensile test results show a comparatively sharp increase in strain rate beyond point T1, with reinforcement tensile rupture only occurring after reaching point T2.

Comparison of the patterns shown in Figs. 8 and 11 suggests that the reinforcement layers did not reach the tensile strength when settlements reached point P1, and that occurred when settlements reached point P2. The higher settlement rate observed after point P1 (in Fig. 8) is attributed to having reached unit tension values that exceed that corresponding to point T1 (in Fig. 11).

Visual inspection of the reinforcement layers retrieved from model F4 supports the assumption that reinforcement failure did not occur for the g-level corresponding to g-level P1. Specifically, Model F4 was tested by increasing the g-level until the monitored settlement at the crest reached 14 mm. This settlement is higher than that corresponding to point P1, but smaller than that corresponding to point P2 (Fig. 8). That is, centrifuge testing of Model F4

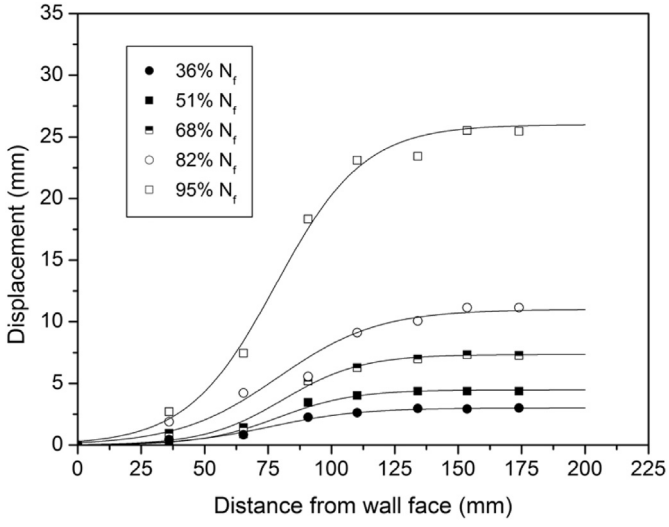

Fig. 9. Displacement data and sigmoid fitting curves for Layer 10 at increasing g-levels (Model F3).

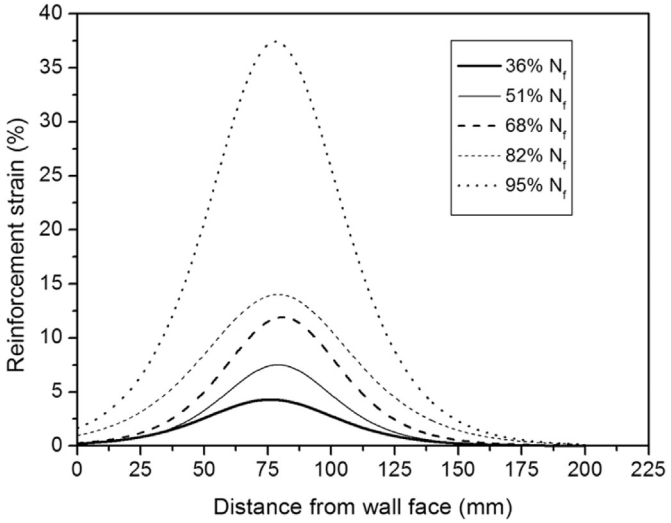

Fig. 10. Strain distribution for Layer 10 at increasing g-levels (Model F3).

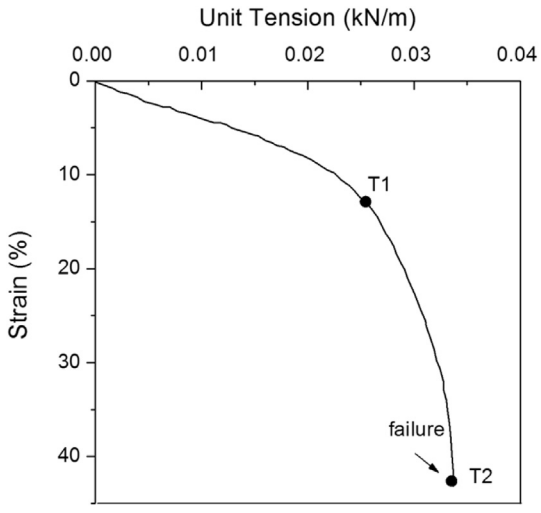

Fig. 11. Typical tensile test results for Geotextile A.

was terminated before reaching final collapse. The objective of this test was to visually assess the characteristics of the geotextile reinforcements after significant straining, but before tensile breakage. After completion of the test, Model F4 was exhumed to examine the reinforcement layers. This inspection indicated that the integrity of the geotextiles had not been compromised by the time the test was terminated. That is, the tears that were characteristic of tensile tests specimens after reaching tensile strength were not observed in the reinforcements retrieved from Model F4. This evaluation provides additional evidence of the appropriateness of the approach adopted to select the g-level at failure. The approach adopted for models built with Geotextile A was also adopted for models built with Geotextile B.

Table 3 shows the g-level at failure obtained for all centrifuge models tested in the "Short-term" series. The g-level at failure (N_f) for each test was determined as the average of the acceleration corresponding to point P_2 and the g-level that resulted in final collapse (i.e. when the failure wedges were observed to slide). The results obtained from repeat models provided almost the same g-level at failure showing that the adopted experimental procedures led to excellent repeatability.

5.1.2. Location of the failure surfaces

Following completion of each "Short-term" test, the reinforcement layers were retrieved to examine the tears and strains in the geotextiles. The reinforcements exhibited a clear break in all the tests conducted in this series, except for Layer 1 in the models. Fig. 12 illustrates the type of failure observed in the retrieved geotextiles after testing. Reinforcement breakage was found to be clearly perpendicular to the direction of loading. Fig. 13 presents the locus of the failure surfaces in the models tested in this series, defined using the locations of geotextile tears observed in models built using Geotextiles A.

Table 3
G-level at failure (N_f) for "Short-term" tests.

Model	g-level at failure (N_f)
F1	20
F2	19
F3	21
F5	48
F6	49

The location of peak strain (i.e. maximum strain) for each reinforcement layer, obtained from the reinforcement strain distributions such as those shown in Fig. 10, was also determined. The location of the failure surface defined using the reinforcement strain distributions was found to show very good agreement with the experimental data collected from the retrieved geotextiles for the various models. Also, the location of failure surfaces obtained for models built with Geotextile A was found to be similar to that obtained for models built with Geotextile B. Finally, the failures surfaces obtained from "Long-term" tests were found to be very similar to those obtained from "Short term" tests.

Overall, the very good agreement obtained between the failure surface defined by geotextile tears and that defined using the location of peak strains provides additional good evidence of the consistency of the experimental data and of the procedure adopted to define the strain distribution in the reinforcement layers.

5.1.3. Reinforcement tension distribution with depth

Current design approaches for reinforced soil walls often consider that the maximum tension among all reinforcements is located towards the toe of the wall. The rationale for this consideration is that reinforcement tension is assumed to be proportional to the horizontal stresses, which in turn increase linearly with depth. However, some studies on geosynthetic-reinforced soil walls have reported that the maximum strain among all reinforcements did not occur towards the toe of the wall (e.g. Simac et al., 1990; Allen et al., 1992; Gourc and Matichard, 1992). This behavior has been attributed to restrictions induced by the foundation as well as to friction between the backfill soil and the wall face.

Although several case histories of instrumented geosynthetic reinforced walls have been reported where the reinforcement tension distribution has been monitored, the structures have been primarily evaluated under working stress conditions. Instead, the centrifuge results presented in this study allows evaluation of the

Fig. 12. View of geotextile reinforcement retrieved after failure of centrifuge model (Model F2, Layer 6).

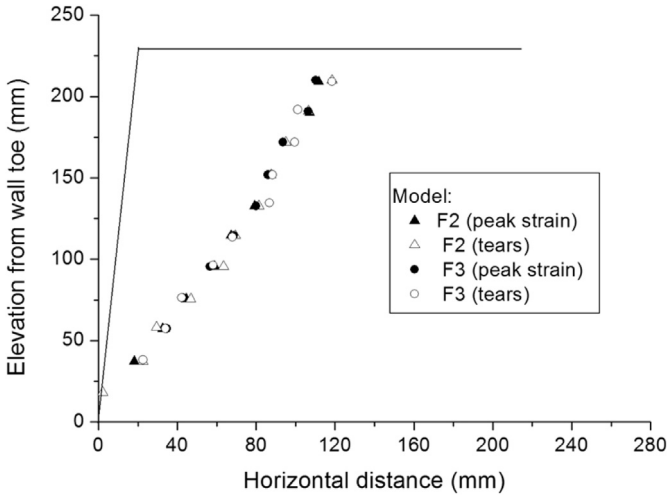

Fig. 13. Location of failure surface after testing of Models F2 and F3.

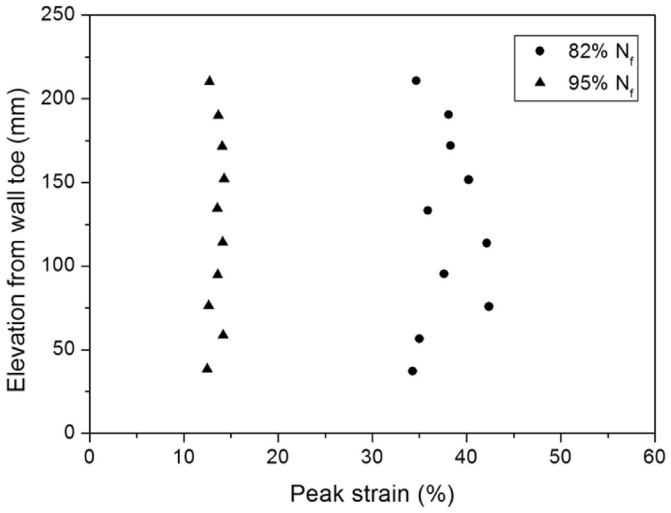

Fig. 14. Distribution of the reinforcement peak strains *versus* elevation (Model F3).

reinforcement tension distribution under significantly higher stress levels, including those near failure conditions.

A review of reported centrifuge studies on reinforced walls was conducted by Arriaga (2003). One such study is the research carried out by Jaber (1989), who instrumented some models in order to obtain tension distribution in a wall reinforced with strips of aluminum foil. The structure initially exhibited a maximum tension distribution growing linearly with depth, except for the two last layers. However, after reaching a g-level of approximately 85% of the g-level at failure, a significant stress redistribution was observed among the reinforcements and, near failure, the maximum load was found to be approximately the same in all reinforcement layers (i.e. reaching a rectangular distribution with depth). Zornberg (1994) and Arriaga (2003) also report that a rectangular tension distribution with depth is more consistent with the patters of rupture observed in centrifuge models involving geotextile reinforced soil slopes.

Fig. 14 illustrates the distribution of maximum strains *versus* elevation from wall toe in each reinforcement layer for Model F3. The peak strain values shown in the figure were predicted using Equation (2) after having defined the sigmoid curves that represent relative displacements in the reinforcement layers. The results in Fig. 14 correspond to comparatively high g-levels. While the magnitude of strains varies with increasing g-levels, a reasonably uniform peak strain with depth can be observed. Similar uniform distributions were also obtained for the other "Short-term" models tested near failure.

The reinforcement tension in each layer (including the maximum reinforcement tension) can be predicted using the strain values in Fig. 14, as follows:

$$T = J \cdot \varepsilon \tag{4}$$

where: T, J and ε, represent the unit tension, geotextile stiffness and strain in the reinforcements, respectively.

The confined value of the geotextile stiffness should be considered in Equation (4), as it has been reported that the geosynthetic stress–strain behavior may be dependent on the soil confinement (e.g. Ling et al., 1992; Ballegeer and Wu, 1993; Mendes et al., 2007; Palmeira, 2009; França and Bueno, 2011). The effect of soil confinement on the mechanical behavior of nonwoven geotextiles has been attributed to a number of mechanisms, including an increased internal friction among fibers and constrained "necking" of the tensioned geotextile. However, these effects are not expected to result in mechanical improvements that increase linearly with confining stress. Indeed, while relevant differences may be expected between the behavior of an unconfined nonwoven geotextile and a nonwoven geotextile under some (perhaps minor) level of confinement, only minor improvements in mechanical properties could be expected (if any) after continued increase in confining stresses. Thus, for the models evaluated in this study, the same value of the confined stiffness was considered, in spite of the different depths of the reinforcement layers. Accordingly, the reinforcement tension could be assumed to be approximately constant with depth for conditions approaching wall failure. This trend is supported by studies performed by Zornberg et al. (1998) and Arriaga (2003) using the same geotextile considered in this study.

It should also be noted that while the most significant variation in stiffness with confinement, for nonwoven geotextiles, has been reported to occur for small strains, for the strain levels of interest in this study (e.g. over 5%), increases in stiffness with confining stress have been reported to be considerably smaller (Christopher et al., 1986). The reinforcement tension distribution with depth is an important outcome from the evaluation of the "Short-term" test series, which is also relevant for the subsequent interpretation of the results from the "Long-term" tests series, discussed next.

5.2. Results from the "Long-term" test series

The tests in the "Long-term" series involved increasing the g-level until a target value and maintaining a constant acceleration. Fig. 15 shows the time-dependent settlements obtained at the top of walls constructed using Geotextiles A, while Fig. 16 shows the settlements with time obtained at the top of walls built with Geotextile B. The time presented in the figures corresponds to the time elapsed after having reached the target acceleration in each test. As shown in the figures, time-dependent settlements were observed to occur in all the tests in this series, with increasing settlement rate for increasing acceleration values. Larger settlements were observed for models constructed using Geotextile B (polypropylene reinforcement) than those constructed with Geotextile A (polyester reinforcement). Models tested using a constant acceleration equal to 80% of the g-level at failure (as defined from "Short-term" tests) resulted in creep rupture. This was specifically observed in models C4 and C8, which failed 4.3 h and 1.8 h, respectively, after having reached the constant target g-level. As in

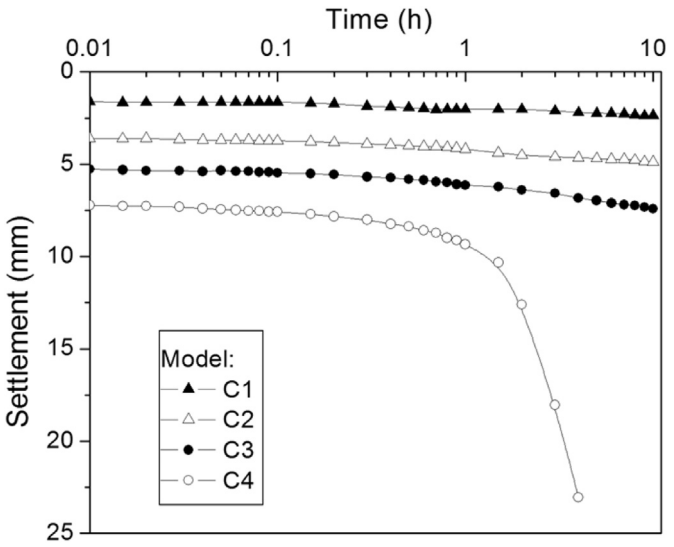

Fig. 15. Time-dependent settlements obtained at the crest of models constructed using Geotextile A ("Long-term" tests).

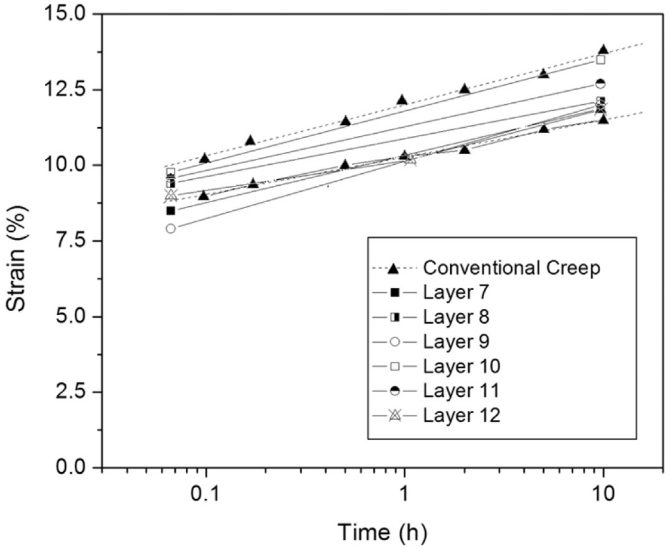

Fig. 17. Time-dependent strains from Geotextile A obtained from Model C3 and from conventional creep tests.

the case of tests in the "Short-term" series, the results from thermocouples placed within the models indicated only minor temperature variations, which were considered negligible for the purposes of this research.

The results shown in Figs. 15 and 16 clearly indicate that the time-dependent characteristics of the reinforcements affected the overall time-dependent performance of the geosynthetic-reinforced wall models. An important aspect evaluated in this study is the suitability of predicting the magnitude of the time-dependent deformations in the reduced-scale models using creep results obtained from geosynthetics tested in isolation. This assessment required initial prediction of the magnitude of the mobilized tension achieved in the reinforcements at the time when the target constant acceleration had been reached in each "Long-term" test. The magnitude of the mobilized tension in each reinforcement layer has often been reported to depend on the elevation of the reinforcement layer. However, as previously discussed, the maximum tension appears to have remained constant with depth, even before rupture. Accordingly, at least for "Long-term" models tested under comparatively high constant acceleration values, the ratio between the target constant acceleration and the g-level at failure (defined from "Short-term" models) was expected to correspond to the ratio between the mobilized reinforcement tension and the tensile strength of the geotextile. In other words, the values of the mobilized geotextile tension in models tested under 25%, 40%, 60% and 80% of g-level at failure was estimated to corresponds to 25%, 40%, 60% and 80%, respectively, of the geotextile tensile strength.

Figs. 17 and 18 present the reinforcement strains obtained in models C3 and C4, which were constructed using Geotextile A as part of the "Long-term" tests series. The tests were conducted under target centrifuge acceleration (N) values corresponding to 60% and 80% of the g-level at failure (N_f). The figures also show the time histories of strains obtained from unconfined creep tests conducted using the same geotextile. As previously mentioned, the scaling

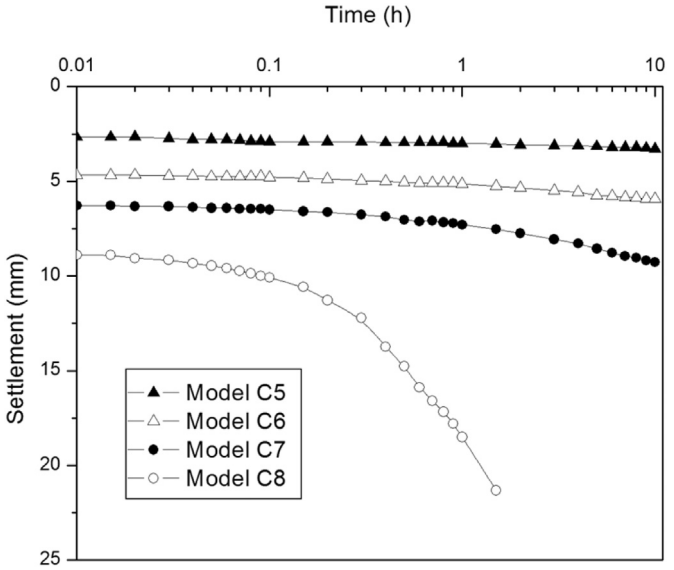

Fig. 16. Time-dependent settlements obtained at the crest of models constructed using Geotextile B ("Long-term" tests).

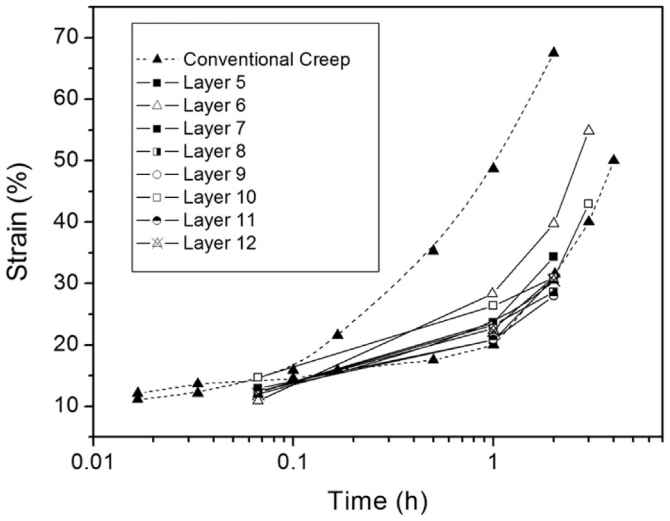

Fig. 18. Time-dependent strains from Geotextile A obtained from Model C4 and from conventional creep tests.

factor for time in creep evaluations of centrifuge testing was considered equal one. It should also be noted that strains presented in these figures correspond to the total strain ε, which includes the following two components:

$$\varepsilon = \varepsilon_i + \varepsilon_{cr} \quad (5)$$

where ε_i is the initial strain value achieved 1 min after rapid loading from an acceleration of 1 g to the target g-level, and ε_{cr} is the subsequent time-dependent creep strain.

The magnitude of the initial strain values presented in Figs. 17 and 18, obtained from geotextiles tested both in isolation and under the confinement of soil (in centrifuge models) shows some variability. However, the magnitude of the initial strains in the centrifuge models is of similar order of magnitude as the strains observed in unconfined tests. For example, the results in Fig. 17 show that the magnitude of initial strains for the different layers (confined specimen) ranged from 7.8% to 9.8%, while a similar range (7.9%–9.7%) is observed for the initial strains for different unconfined tests. The observed differences in the initial strain component ε_i could also be attributed to differences between the rate of the loading to achieve the target load in conventional creep tests (target load is achieved in approximately 1 min) and the comparatively longer time required to reach the target g-level in the centrifuge models (around 30 min). However, it should be noted that in spite of some variability in ε_i, very good consistency was obtained among the results for creep strains, ε_{cr}, as observed in Figs. 17 and 18. In particular, while the initial loading rate may have influenced the initial strains, creep rates tend to exhibit similar values over time (Allen and Bathurst, 2002a). Good consistency was also observed for time to creep rupture between confined and unconfined specimens. Specifically, time to failure for the centrifuge model tested under 80% of the g-level at failure was approximately 4 h, which is well within the range of times to failure obtained from unconfined tests (1–5 h).

Figs. 19 and 20 present the reinforcement strains obtained in Models C7 and C8, which were constructed using Geotextile B, as part of the "Long-term" test series. Also in this case, the figures show the strains with time obtained from unconfined creep tests. Although initial strains were smaller in the models, possibly due to the confinement effect, the magnitude of the confined creep strain rates were also found to be remarkably similar to the unconfined creep strains. In terms of time to failure, the results were also found to be very consistent, with times to failure ranging from 53 min to 1.6 h in conventional creep tests and occurring in 1.8 h in the confined (centrifuge) specimens that reached failure.

The similarity between the geotextile time-dependent deformations obtained in the centrifuge models and in the specimens tested in-isolation is remarkable, particularly considering that the reinforcements used in this study are nonwoven geotextiles. However, it should be noted that while previous studies have reported that confinement may affect creep results in nonwoven geotextiles (e.g. Levacher et al., 1994), the reported effects were not as significant as those reported for the geotextile tensile properties.

It should be emphasized that the consistency in the magnitude and rate of time-dependent strains obtained in this study for confined geotextiles (in centrifuge models) and in conventional creep tests required consistency in the selection of the reference tensile values. Specifically, creep load levels are generally reported as a fraction of the geotextile tensile strength. Accordingly, the load levels in conventional unconfined creep tests were defined as a fraction of the geotextile *unconfined* tensile strength. However, the load levels in the model reinforcements were defined as a fraction of the geotextile *confined* tensile strength. This is because the g-level for the "Long-term" models was defined as a percentage of g-level at failure obtained from "Short-term" tests since failure in the "Short-term" tests only occurred after geotextiles have reached the *confined* tensile strength. Thus, the consistency of load levels (i.e. as a fraction of *unconfined* strength for geotextiles in conventional creep tests, but as a fraction of *confined* strength for geotextiles in centrifuge the models) justifies the good agreement between the results from unconfined and confined geotextiles shown in Figs. 17 and 18.

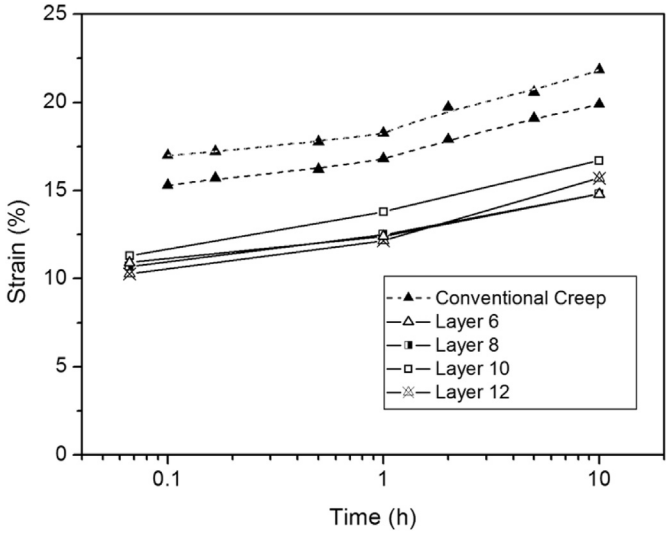

Fig. 19. Time-dependent strains from Geotextile B obtained from Model C7 and from conventional creep tests.

6. Implications of the results

The results of the centrifuge tests indicate that the magnitude of time-dependent creep strains developed in the centrifuge models, under sand confinement, was similar to that obtained from conventional creep tests. While experimental data have not been fully available in the technical literature, it has been expected that the creep characteristics of confining granular soils may result in smaller time-dependent deformations than those quantified using

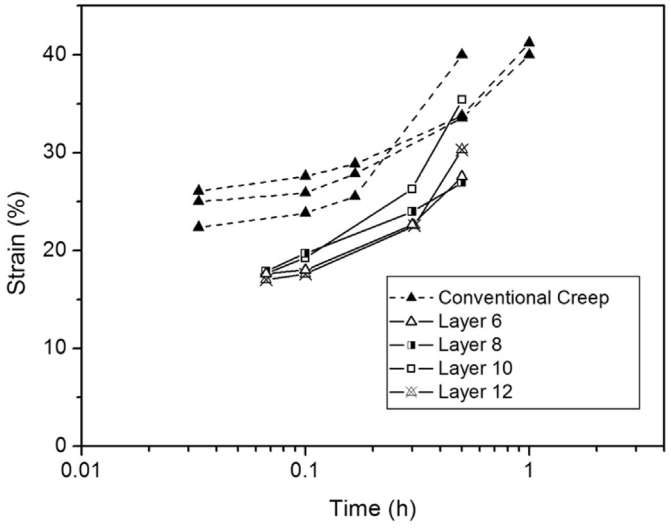

Fig. 20. Time-dependent strains from Geotextile B obtained from Model C8 and from conventional creep tests.

geosynthetic products tested in isolation. This is because granular soils have been considered to have negligible creep. However, it should be noted that the creep rate of sands in typical GRS walls may not be as limited as often considered. Based on the evaluation of full-scale instrumented walls, typically reported values for the maximum reinforcement strains are small, ranging from 0.5% to 3%. While this magnitude of strains corresponds to comparatively low levels of mobilized reinforcement tension, it may result in comparatively high levels of mobilized soil shear stress. Allen and Bathurst (2002b), for example, evaluated full-scale instrumented walls and reported that level of reinforcement loads ranged from 1% to 7% of the reinforcement ultimate tensile strength. Accordingly, any qualitative comparison between the creep strain rates of soil and reinforcement should consider comparatively low tension levels in the reinforcement but comparatively high stress levels in the soil.

For illustration purposes, creep strain rates for different geosynthetics reported in the technical literature are presented in Fig. 21. The curves were obtained using conventional creep tests results, with each curve corresponding to a different geosynthetic specimen subjected to constant load. The load level is identified in the figure as a fraction of its ultimate tensile strength (T_{ult}). For a given geosynthetic, the creep strain rates increase with increasing load levels. Fig. 21 also presents the creep strain rates for Geotextiles A and B, which were defined using the results from conventional creep tests. If the results of multiple creep tests are available for a given load level (e.g. tests for 60% of T_{ult}, as reported in Figs. 5 and 7) the average of creep rates from multiple tests are presented in Fig. 21). As shown in the figure, the creep strain rates of the geotextile simulants used as reinforcement in the centrifuge models are consistent with those reported in the literature for geosynthetics used in reinforced soil structures.

Creep rates that were considered typical for sands by Kuhn and Mitchell (1993) are shown in Fig. 22. Each line in the figure corresponds to the shear strain rates ($d\gamma/dt$) obtained from the results of triaxial tests conducted by Murayama et al. (1984). These results correspond to comparatively high levels of constant deviator stresses. The soil creep results presented in the figure indicate that the strain rates show a linear trend, when using logarithmic scales, which is consistent with the trends observed for geosynthetics. The levels of constant stress are defined as a fraction of the estimated ultimate soil shear strength (τ_{max}). For comparison, Fig. 22 also shows the upper and lower bounds of the geosynthetic creep strain rates shown in Fig. 21.

The results in Fig. 22 indicate that it is feasible that similar creep strain rates be developed in the granular soils and in the geosynthetic reinforcements of GRS walls. This is particularly relevant when considering that the reinforcement load levels in full-scale instrumented GRS walls are typically smaller than those indicated in Fig. 22. While the soil shear stress levels may be higher than those shown in the figure (e.g. 100% of τ_{max} when reaching an active state of stresses).

The soil used in the centrifuge models in this study, frequently considered as having negligible creep, was ultimately found not to prevent the development of time-dependent deformations. Indeed, the results of tests under higher g-levels resulted in creep rupture of the geotextiles, which is a mechanism that has not been previously reported, under the confinement of soil, in the technical literature. The results of this study suggest that the creep reduction factors may not be reduced by merely considering a smaller tendency to creep of confining granular soils. Indeed, time-dependent deformations were found to develop for all the acceleration levels considered in this study. Overall, the results from this centrifuge study provide experimental evidence of relevance of accounting for creep in geosynthetic-reinforced walls design, even when using granular materials as backfill.

7. Conclusions

Centrifuge tests were performed to investigate the time-dependent deformations in geotextile-reinforced soil walls. The models were built using nonwoven fabrics as reinforcement elements and dry sand as backfill material. In some tests, designated herein as “Short-term” tests, the models were loaded to failure by steadily increasing the centrifugal acceleration. In a second series of tests, the “Long-term” tests, the models were subjected to a constant acceleration and their time-dependent deformations were monitored. The following conclusions can be drawn from analysis of the experimental results obtained in this study:

- Settlement measurements at the crest of the models conducted as part of the “Short-term” test series showed good

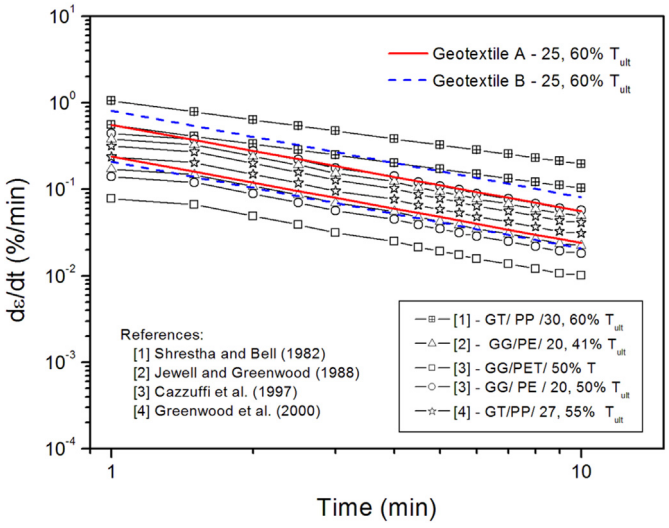

Fig. 21. Creep strain rate for geosynthetics reported in literature, as well as for those used in this study (Note: GT – geotextile, GG – geogrid, PP – polypropylene, PE – polyethylene, PET – polyester).

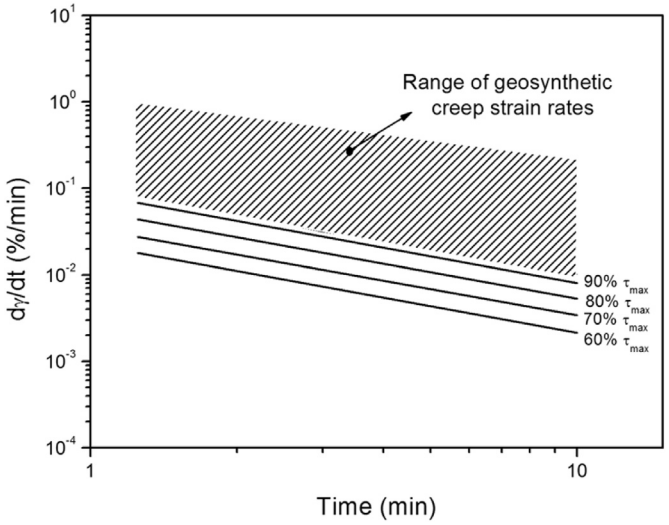

Fig. 22. Typical creep shear strain rates based on Murayama et al. (1984). Note: the range of strain rates for geosynthetics (from Fig. 21) is shown for comparative purpose.

repeatability. Also, the locations of geotextile tears observed after dissection of the "Short-term" tests indicated very good agreement with the failure surfaces obtained based on the locations of the reinforcement peak strains. These results provide good evidence of the consistency of the centrifuge experimental data including the g-level at failure defined using results from the "Short-term" tests.

- Results from "Short term" tests indicate that significant stresses redistribution occurs among reinforcement layers, and that particularly at higher g-levels, the maximum reinforcement tension reaches an approximately uniform distribution with depth.
- Even though the models were constructed using sand as backfill material, which is often expected to show negligible creep, all "Long-term" tests performed in this study showed relevant time-dependent deformations, as evidenced by time-dependent settlements at the crest of the "Long-term" models as well as time-dependent strains in the reinforcements.
- The magnitude and rate of time-dependent strains in confined geotextiles (from centrifuge models) were found to be remarkably similar to the magnitude and rate of time-dependent strains in unconfined geotextiles from conventional creep.
- The centrifuge results indicated that the creep behavior of geotextiles may even lead to creep failure of geosynthetic-reinforced walls, as observed in models that have been subjected to an acceleration equal to 80% of the g-level at failure. The time to creep failure for centrifuge models was found to compare well with the range of times to failure obtained in unconfined tests.
- The soil used in the models, a uniform sand, was found not to restrain the development of time-dependent deformations in the reinforcements nor the long-term rupture of geotextiles in the models. This indicates that the current practice of penalizing the reinforcement ultimate tensile strength using significant creep reduction factors may not be as overly conservative as sometimes speculated. That is, the results of this study suggest that the creep reduction factors may not be reduced by considering the supposedly smaller tendency to creep of a confining granular soil.

These conclusions are based on the materials and test conditions used in this study, which include the use of specific backfill (uniform sand), a specific reinforcement vertical spacing as well as stress levels that are beyond working stress conditions. Overall, the experimental data generated in this study indicates that significant time-dependent deformations can occur in geosynthetic-reinforced wall systems, even if constructed with granular backfill. Consequently, although currently available design methods for reinforced soil walls have been deemed conservative, any reassessment of current design approaches should not minimize that possibly significant time-dependent deformations, and even failure, that may result if reinforcements are loaded to comparatively high tension levels.

Acknowledgments

The first author is grateful by the support provided by Brazilian Research Agency CAPES (BEX 0602/02-7).

References

Allen, T.M., Christopher, B.R., Holtz, R.D., 1992. Performance of a 12.6 m high geotextile wall in Seattle, Washington. In: Proceedings of International Symposium on Geosynthetic-reinforced Soil Retaining Walls, Denver, USA, pp. 81–100.

Allen, T.M., Bathurst, R.J., 2002a. Observed long-term peformance of geosynthetic wall and implications for design. Geosynth. Int. 9 (5–6), 567–606.

Allen, T.M., Bathurst, R.J., 2002b. Soil reinforcement loads in geosynthetics walls at working stress conditions. Geosynth. Int. 9 (5–6), 525–566.

Arriaga, F., 2003. Response of Geosynthetic-reinforced Structures under Working Stress and Failure Conditions (Ph.D. Thesis). University of Colorado at Boulder, Boulder, Colorado, USA, 205 pages.

ASTM D 4253, 2014. Standard Test Methods for Maximum Index Density and Unit Weight of Soils Using a Vibratory Table. American Standard Testing Materials International, West Conshohocken, Pennsylvania, USA, 14 pages.

ASTM D 4254, 2014. Standard Test Methods for Minimum Index Density of Soils and Calculation of Relative Density. American Standard Testing Materials International, West Conshohocken, Pennsylvania, USA, 9 pages.

ASTM D 4595, 2011. Standard Test Method for Tensile Properties of Geotextiles by the Wide-width Strip Method. American Standard Testing Materials International, West Conshohocken, Pennsylvania, USA, 13 pages.

ASTM D 5262, 2012. Standard Test Method for Evaluating the Unconfined Tension Creep Behavior of Geosynthetics. American Standard Testing Materials International, West Conshohocken, Pennsylvania, USA, 16 pages.

Ballegeer, J.P., Wu, J.T.H., 1993. Intrinsic confined and unconfined load-deformation properties of geotextiles. In: Cheng, S.J.C. (Ed.), Geosynthetics Soil Reinforcement Testing Procedures, Philadelphia, USA, pp. 16–31.

Bathurst, R.J., Benjamim, D.J., 1990. Failure of a geogrid-reinfocred soil wall. Transp. Res. Rec. 1288, 109–118.

Bathurst, R.J., Jarrett, P.M., Benjamim, D.J., 1993. A database of results from an incrementally constructed geogrid-reinforced soil wall test. In: Proceedings of Soil Reinforcement: Full Scale Experiments of the 80s, Paris, France, pp. 401–430.

Bueno, B.S., Constanzi, M.A., Zornberg, J.G., 2005. Conventional and accelerated creep tests on nonwoven needle-punched geotextiles. Geosynth. Int. 12 (6), 276–287.

Cazzuffi, D., Ghinelli, A., Sacchetti, M., Villa, C., 1997. European experimental approach to the tensile creep behavior of high-strength geosynthetics. In: Proceedings of Geosynthetics', vol. 1, pp. 253–266. California, USA.

Christopher, B.R., Holtz, R.D., Bell, W.D., 1986. New tests for determining the in-soil stress-strain properties of geotextiles. In: Proceedings of the Third International Conference on Geotextiles, vol. 3, pp. 683–688. Vienna, Austria.

França, F.A.N., Bueno, B.S., 2011. Creep behavior of geosynthetics using confined accelerated tests. Geosynth. Int. 18 (5), 242–254.

Gourc, J., Matichard, Y., 1992. Development of geotextile reinforcement techniques in France – application to retaining structures. In: Proceedings of International Symposium on Geosynthetic-reinforced Soil Retaining Walls, Denver, USA, pp. 131–152.

Greenwood, J.H., Kempton, G.T., Watts, G.R.A., Bush, D.I., 2000. Twelve year creep tests on geosynthetic reinforcement. In: Proceedings of the Second European Geosynthetics Conference – EuroGeo, vol. 1, pp. 333–336. Bologna, Italy.

Helwany, S.M.B., Shin, S., 1998. Creep and stress relaxation of geotextile-reinforced soils. Geosynth. Int. 5 (4), 425–434.

Jaber, M.B., 1989. Behavior of Reinforced Soil Walls in Centrifuge Model Tests. Berkeley (Ph.D. Thesis). University of California, Berkeley, USA, 239 pages.

Jewell, R.A., Greenwood, J.H., 1988. Long term strength and safety in steep soil slopes reinforced by polymer materials. Geotext. Geomemb. 7 (1–2), 81–118.

Jones, C.J.F.P., Clarke, D., 2007. The residual strength of geosynthetic reinforcement subjected to accelerated creep testing and simulated seismic events. Geotext. Geomemb. 25 (3), 155–169.

Ketchart, K., Wu, J.T.H., 2002. A modified soil-geosynthetic interactive performance test for evaluating deformation behavior of GRS structures. Geotech. Test. J. 25, (4), 1–9.

Kongkitkul, W., Tatsuoka, F., 2007. A theoretical framework to analyse the behaviour of polymer geosynthetic reinforcement in temperature-accelerated creep tests. Geosynth. Int. 14 (1), 23–38.

Kongkitkul, W., Tatsuoka, F., Hirakawa, D., Sugimoto, T., Kawahata, S., Ito, M., 2010. Time histories of tensile force in geogrid arranged in two full-scale high walls. Geosynth. Int. 17 (1), 12–33.

Kongkitkul, W., Chantachot, T., Tatsuoka, F., 2014. Simulation of geosynthetic load–strain–time behaviour by the non-linear three-component model. Geosynth. Int. 21 (4), 244–255.

Kuhn, M.R., Mitchell, J.K., 1993. New perspectives on soil creep. J. Geotech. Eng. 119 (3), 507–523.

Levacher, D., Blivet, J.C., Msouti, F., 1994. Tensile and creep behavior of geotextiles. In: Proceedings of the Fifth International Conference on Geotextiles, Geomembranes and Related Products, vol. 3, pp. 1131–1134. Singapore.

Li, F.-L., Peng, F.-L., Tan, Y., Kongkitkul, W., Siddiquee, M.S.A., 2012. FE simulation of viscous behavior of geogrid-reinforced sand under laboratory-scale plane-strain-compression testing. Geotext. Geomemb. 31, 72–80.

Ling, H.I., Wu, J.T.H., Tatsuoka, F., 1992. Short-term strength and deformation characteristics of geotextiles under typical operational conditions. Geotext. Geomemb. 11 (2), 185–219.

Liu, H., Wang, X., Song, E., 2009. Long-term behavior of GRS retaining walls with marginal backfill soils. Geotext. Geomemb. 27, 295–307.

McGown, A., Andrawes, K.Z., Kabir, M.H., 1982. Load-extension testing of geotextiles confined in soil. In: Proceedings of the Second International Conference on Geotextiles, vol. 3, pp. 793–798. Las Vegas, USA.

Mendes, M.J.A., Palmeira, E.M., Matheus, E., 2007. Some factors affecting the in-soil load–strain behaviour of virgin and damaged nonwoven geotextiles. Geosynth. Int. 14 (1), 39–50.

Mitchell, J.K., Jaber, M., Shen, C.K., Hua, Z.K., 1988. Behavior of Reinforced Soil Walls in Centrifuge Model Tests. In: Proceedings of Centrifuge '88, Paris, France, pp. 259–271.
Murayama, S., Michihiro, K., Sakagami, T., 1984. Creep characteristics of sands. Soils Found. 24 (2), 1–15.
Palmeira, E.M., 2009. Soil–geosynthetic interaction: modelling and analysis. Geotext. Geomemb. 27, 368–390.
Shrestha, S.C., Bell, J.R., 1982. Creep behavior of geotextiles under sustained loads. In: Proceedings of the Second International Conference on Geotextiles, vol. 3, pp. 769–774. Las Vegas, USA.
Simac, M.R., Christopher, B.R., Bonczkiewicz, C., 1990. Instrumented field performance of a 6 m geogrid soil wall. In: Geotextiles, Geomembranes and Related Products, Balkema, vol. 1, pp. 53–59. Rotterdam.
Wu, C.S., Hong, Y.S., 1994. Creep behavior of geotextile under confining stress. In: Proceedings of the Fifth International Conference on Geotextiles, Geomembranes and Related Products, vol. 3, pp. 1135–1138. Singapore.
Wu, J.T.H., Helwany, S.M.B., 1996. A performance test for assessment of long-term creep behavior of soil-geosynthetic composites. Geosynth. Int. 3 (1), 107–124.
Yeo, S.-S., Hsuan, Y.G., 2010. Evaluation of creep behavior of high density polyethylene and polyethylene-terephthalate geogrids. Geotext. Geomemb. 28, 409–421.
Zornberg, J.G., 1994. Performance of Geotextile-reinforced Soil Structures (Ph.D. Thesis). University of California, Berkeley, California, USA.
Zornberg, J.G., Mitchell, J.K., Sitar, N., 1997. Testing of reinforced slopes in a geotechnical centrifuge. Geotech. Test. J. 20 (4), 470–480.
Zorneberg, J.G., Sitar, N., Mitchell, J.K., 1998. Limit equilibrium as basis for design of geosynthetic-reinforced slopes. J. Geotech. Geoenviron. Eng. 124 (8), 684–698.
Zornberg, J.G., Arriaga, F., 2003. Strain distribution within geosynthetic-reinforced slopes. J. Geotech. Geoenviron. Eng. 129 (1), 32–45.
Zornberg, J.G., Byler, B.R., Knudsen, J., 2004. Creep of geotextiles using time-temperature superposition methods. J. Geotech. Geoenviron. Eng. 130 (11), 1158–1168.